

# Investigation of the Lightest Hybrid Meson Candidate with a Coupled-Channel Analysis of $\bar{p}p$ -, $\pi^-p$ - and $\pi\pi$ -Data

B. Kopf, M. Albrecht, H. Koch, J. Pychy, X. Qin,\* and U. Wiedner  
*Ruhr-Universität Bochum, 44801 Bochum, Germany*

Based on new insights from two recent coupled-channel analyses of  $\bar{p}p$  annihilation together with  $\pi\pi$ -scattering data and of  $\pi^-p$  data, this paper aims at a better understanding of the spin-exotic  $\pi_1$  resonances in the light meson sector. The Crystal Barrel Collaboration observed the  $\pi_1$ -wave in  $\bar{p}p$  annihilations in flight for the first time with the coupling to  $\pi^0\eta$  in the reaction  $\bar{p}p \rightarrow \pi^0\pi^0\eta$  with a sophisticated coupled-channel approach. Another refined coupled-channel analysis of the P- and D-waves in the  $\pi\eta$  and  $\pi\eta'$  system based on data measured at COMPASS has been performed by the JPAC group. In that study the two spin-exotic signatures listed in the PDG, the  $\pi_1(1400)$  and  $\pi_1(1600)$ , with a separate coupling to  $\pi\eta$  and  $\pi\eta'$  can be described by a single pole. In this paper, both analyses, the one with the three  $\bar{p}p$  annihilation channels into  $\pi^0\pi^0\eta$ ,  $\pi^0\eta\eta$  and  $K^+K^-\pi^0$  and 11 different  $\pi\pi$ -scattering data sets and the one with the P- and D-wave data in the  $\pi\eta$  and  $\pi\eta'$  systems measured at COMPASS, are subjected to a combined coupled channel analysis. By utilizing the K-matrix approach and realizing the analyticity via Chew-Mandelstam functions the  $\pi_1$  wave can be well described by a single pole for both systems,  $\pi\eta$  and  $\pi\eta'$ . The mass and width of the  $\pi_1$ -pole are measured to be  $(1561.6 \pm 3.0^{+6.6}_{-2.6})$  MeV/ $c^2$  and  $(388.1 \pm 5.4^{+0.2}_{-14.1})$  MeV.

## I. INTRODUCTION

The picture of  $\pi_1$  hybrids with spin-exotic quantum numbers  $I^G(J^{PC}) = 1^-(1^{-+})$  in the light meson sector is poorly understood and the experimental indications of various resonances are controversially discussed. Lattice calculations [1–3] and phenomenological QCD studies [4, 5] predict only one state at a mass of 2 GeV/ $c^2$  or slightly below. Experimentally, three different resonances with  $I^G(J^{PC}) = 1^-(1^{-+})$  quantum numbers are reported. The lightest one, the  $\pi_1(1400)$ , has only been seen in the  $\eta\pi$  decay mode by several experiments [6–12]. For the  $\pi_1(1600)$  instead, no coupling to  $\eta\pi$  has been found, but it has been observed in several other channels, namely  $\pi\eta'$ ,  $\rho\pi$ ,  $f_1(1285)\pi$  and  $b_1(1235)\pi$  [13–18]. The third state which has the poorest evidence, and is thus not listed in the PDG, is the  $\pi_1(2015)$  probably seen decaying into  $f_1(1285)\pi$  and  $b_1(1235)\pi$  [16, 17]. A weak point in various of these old analyses was the extraction of the resonance parameters by making use of Breit-Wigner parameterizations. The outcome of a recent analysis likely shed more light on the understanding of the light  $\pi_1$  hybrids [19]. Utilizing the N/D method for the dynamics, it turned out that the  $\pi_1(1400)$  and  $\pi_1(1600)$ , with a separate coupling to  $\pi\eta$  and  $\pi\eta'$  can be described by only one pole.

The Crystal Barrel Collaboration very recently observed the  $\pi_1$ -wave in  $\bar{p}p$  annihilations in flight for the first time with a coupling to  $\pi\eta$  in the reaction  $\bar{p}p \rightarrow \pi^0\pi^0\eta$  [20] using a coupled-channel analysis. In the study presented here, this analysis has been extended by considering not only the channels  $\bar{p}p \rightarrow \pi^0\pi^0\eta$ ,  $\pi^0\eta\eta$  and  $K^+K^-\pi^0$  at a beam momentum of 900 MeV/ $c$  and data

from 11 different  $\pi\pi$ -scattering channels but also the P- and D-waves in the  $\pi\eta$  and  $\pi\eta'$  systems measured at COMPASS [19]. The dynamics is treated slightly differently compared to [21]. The K-matrix approach was used by taking into account the analyticity with Chew-Mandelstam functions [22].

## II. PARTIAL WAVE ANALYSIS

The partial wave analysis has been performed with the software package PAWIAN (**P**artial **W**ave **I**nteractive **A**nalysis Software) [23] and with the same algorithms as described in [20].

*Description of the  $\bar{p}p$  channels:* The data used in the analysis are the three  $\bar{p}p$  annihilation channels  $\pi^0\pi^0\eta$ ,  $\pi^0\eta\eta$  and  $K^+K^-\pi^0$  at a beam momentum of 900 MeV/ $c$  measured with the Crystal Barrel detector at LEAR. The full description of the reconstruction and event selection can be found in [20].

The complete reaction chain starting from the  $\bar{p}p$  initial state down to the final state particles is fitted. The description for the amplitudes of the non-dynamical part is based on the helicity formalism. The amplitudes are further expanded into the LS-scheme which guarantees that also the orbital momentum dependent barrier factors for the production and the decay can be properly considered. In addition to  $\pi_1\pi^0$  the sub-channels  $f_0\eta$ ,  $f_2\eta$ ,  $a_0\pi^0$  and  $a_2\pi^0$  are contributing to  $\bar{p}p \rightarrow \pi^0\pi^0\eta$ . The contributing isovector states  $a_0$  and  $a_2$  exhibit a similar decay pattern as the  $\pi_1$ -wave with a strong coupling to the  $\pi^0\eta$  system. Therefore it is not straightforward to properly disentangle these waves from each other. In this case, the simultaneous fit of the channels  $\pi^0\eta\eta$  and  $K^+K^-\pi^0$  helps considerably. It ensures a strong control on the production of  $a_0\pi^0$  and  $a_2\pi^0$  by directly sharing the relevant amplitudes between the two channels

\* Now at Shandong University, 266237 Qingdao, China

$\pi^0\pi^0\eta$  and  $K^+K^-\pi^0$ . Apart from the two isolated resonances  $\phi(1020)$  and  $K^*(892)^\pm$  which are described by Breit-Wigner functions the K-matrix formalism with P-vector approach is used for the dynamics [20].

For each partial wave with defined quantum numbers  $I^G(J^P)$  the mass dependent amplitude  $F_i^P(s)$  is parametrized as follows:

$$F_i^P(s) = \sum_j (I - K(s) C(s))_{ij}^{-1} \cdot P_j^P(s), \quad (1)$$

where  $i$  and  $j$  represent the two body decay channels like  $\pi\pi$ ,  $\pi\eta$  or  $K^+K^-$ .  $s$  is the invariant mass squared of the respective two body sub-channel. The analyticity is considered by the Chew-Mandelstam function  $C(s)$  [22].  $P_j^P(s)$  represents one element of the P-vector taking into account the production process  $p$ :

$$P_j^P(s) = \sum_\alpha \left( \frac{\beta_{\alpha p}^P g_{\alpha j}^{bare}}{m_\alpha^{bare 2} - s} + \sum_k c_{ki} \cdot s^k \right) \cdot B^l(q_j, q_{\alpha_j}), \quad (2)$$

where  $\beta_{\alpha p}^P$  is the complex parameter representing the strength of the produced resonance  $\alpha$ .  $m_\alpha^{bare}$  is the bare mass of the resonance  $\alpha$ .  $B^l(q_j, q_{\alpha_j})$  denotes the Blatt-Weisskopf barrier factor of the decay channel  $j$  with the angular momentum  $l$ , the breakup momentum  $q_j$  and the resonance breakup momentum  $q_{\alpha_j}$ . It is worth mentioning that the production barrier factors are already taken into account separately in the production amplitude as described in [20]. The  $s$  dependent polynomial terms of the order  $k$  with the parameters  $c_{ki}$  describe background contributions for the production.

The elements of the K-matrix for the two body scattering process with angular momentum  $l$  are given by

$$K_{ij}(s) = \sum_\alpha B^l(q_i, q_{\alpha_i}) \cdot \left( \frac{g_{\alpha i}^{bare} g_{\alpha j}^{bare}}{m_\alpha^{bare 2} - s} + \tilde{c}_{ij} \right) \cdot B^l(q_j, q_{\alpha_j}), \quad (3)$$

where  $i$  and  $j$  represent the input and output channels, respectively. The parameters  $\tilde{c}_{ij}$  stand for the constant terms of the background contributions, which are allowed to be added to the K-matrix without violating unitarity. In addition to the form given in Eq. (3), the K-matrix elements for the description of the  $f_0$  wave are multiplied with an Adler zero term as outlined in detail in [20].

The K-matrix descriptions of the  $f_0$ -,  $f_2$ -,  $\rho$ -,  $a_0$ - and  $(K\pi)_{S^-}$  waves are the same as described in [20]. A slightly different K-matrix for the  $\pi_1$ - and  $a_2$ -wave has been used:

- the  $\pi_1$ -wave consists of 1 K-matrix pole and the two channels  $\pi\eta$  and  $\pi\eta'$ . Constant background terms for the K-matrix and the P-vector for the  $\bar{p}p$  channel have been used. Due to the fact that the t-channel exchange plays an important role for the  $\pi^-p$ -scattering process, a first order polynomial is needed for the relevant background terms of these P-vector elements.

- the K-matrix of the  $a_2$ -wave is described by two poles,  $a_2(1320)$  and  $a_2(1700)$ , and by the 3 channels  $\pi\eta$ ,  $\pi\eta'$  and  $K\bar{K}$ . Constant background terms for the K-matrix are used. No background terms for the P-vector are needed for the  $\bar{p}p$  channels while also here first order polynomial background terms are required for the production in  $\pi^-p$ .

This is due to the fact that the COMPASS data are simultaneously fitted, which contain not only the  $\pi\eta$ , but also the  $\pi\eta'$  channel.

*Description of the  $\pi\pi$ -scattering data:* The mass dependent terms of each partial wave of the  $\pi\pi$ -scattering reactions are described by the T-matrix

$$T(s) = (I - K(s) C(s))^{-1} K(s), \quad (4)$$

where  $s$  is the total energy squared. For elastic channels phase and inelasticity are compared with the data. For inelastic channels, like  $\pi\pi \rightarrow \eta\eta$ , the moduli squared of the T-matrix are taken. As in [20] the following data for the  $I = 0$   $S$ - and  $D$ -wave and the  $I = 1$   $P$ -wave for energies below  $\sqrt{s} < 1.9 \text{ GeV}/c^2$  were included in the analysis:

- the phases and inelasticities of the reaction  $\pi\pi \rightarrow \pi\pi$  for the  $I = 0$   $S$ - and  $D$ -wave and for the  $I = 1$   $P$ -wave,
- the intensities of the inelastic channels  $\pi\pi \rightarrow K\bar{K}$  and  $\pi\pi \rightarrow \eta\eta$  for the  $I = 0$   $S$ - and  $D$ -wave and
- the intensity of the inelastic channel  $\pi\pi \rightarrow \eta\eta'$  for the  $I = 0$   $S$ -wave.

*Description of the COMPASS data:* The COMPASS data are taken from the mass independent analysis of  $\pi p \rightarrow \eta^{(\prime)}\pi p$  with a 190 GeV pion beam integrated over the transferred momentum squared  $-t_1$  between 0.1 and 1.0  $\text{GeV}^2$  [19]. Only the intensities of the P- and D- wave and their relative phase for the two channels  $\pi\eta$  and  $\pi\eta'$  are considered. The choice of these waves for the coupled-channel analysis ensures strong constraints in particular for the channel  $\pi^0\pi^0\eta$ , where large contributions of the  $\pi_1$  and  $a_2$  waves are found.

The description of the reaction  $\pi p \rightarrow R p \rightarrow (\eta^{(\prime)}\pi)p$  with R being the produced  $\pi_1$  or  $a_2$  resonances is approximated via the exchange of a Pomeron with  $J^P = 1^-$  and an effective transferred momentum squared of  $t_{eff} = -0.1 \text{ GeV}^2$ . The fits to the intensities of the COMPASS data for the P- and D-wave  $I_{\pi\eta^{(\prime)}}^{\pi p}$  are described by:

$$I_{\pi\eta^{(\prime)}}^{\pi p} = p_{\pi\eta^{(\prime)}}^{2J-2} \cdot q_{\pi\eta^{(\prime)}} \cdot |F_{\pi\eta^{(\prime)}}^{\pi p}|^2 \quad (5)$$

where  $J$  stands for the spin of the relevant  $F$ -vector wave,  $q_{\pi\eta^{(\prime)}}$  for the  $\pi\eta^{(\prime)}$  breakup momentum representing the behavior of the phase space for the decay and  $p_{\pi\eta^{(\prime)}}$  is the  $\pi$  beam momentum in the  $\pi\eta^{(\prime)}$  rest frame.  $F_{\pi\eta^{(\prime)}}^{\pi p}$  and  $P_l^{\pi p}$  are taken as given in Eq. (1) and Eq. (2), respectively. The production barrier factor is considered by

$p_{\pi\eta^{(\prime)}}^{2J-2}$  according to [21, 24], where  $p_{\pi\eta^{(\prime)}} = \frac{\sqrt{\lambda(s, m_{\pi}^2, t_{eff})}}{2\sqrt{s}}$  is the production breakup momentum with  $\lambda$  being the Källén triangle function.

The phases for the  $\pi_1$  and  $a_2$ -waves for the channels  $\pi\eta$  and  $\pi\eta'$  are calculated as defined in Eq. (1) by the phase angles of the  $F_{\pi\eta^{(\prime)}}^{\pi p}$ -vector projected to the relevant channel.

A combined minimization function is used for the fit, in which all data sets are considered. While for the  $\bar{p}p$  data the full information of each event in the multi-dimensional phase space volume is utilized, the other data sets are provided as one-dimensional data points with errors. The construction of the complete likelihood and minimization function is performed analogously to [20] and described in detail therein.

Detailed studies have shown that the significantly best fit result is achieved with the same hypothesis which was also preferred to be the best one in [20].

### III. FIT RESULT

Good agreement is achieved between the fit based on the best hypothesis summarized above and all data samples. Exemplarily for all  $\bar{p}p$  channels, the result for  $\pi^0\pi^0\eta$  is shown in Fig. 1. The invariant  $\pi^0\eta$  mass as well as the production and decay angular distribution of the subsys-

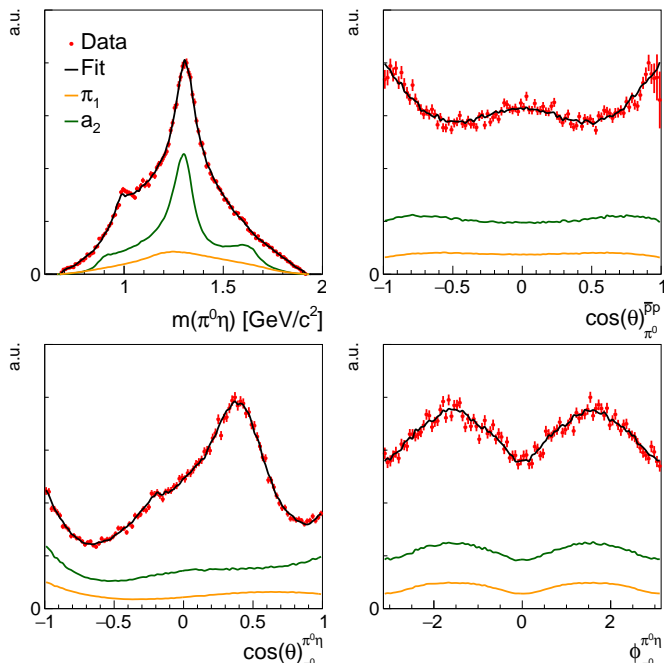


FIG. 1. Invariant mass distribution (upper left) and selected angular distributions for the production (upper right) and decay (lower left and right) of the  $\pi^0\pi^0\eta$  channel. The red markers with error bands show the efficiency corrected data with two entries per event, while the black line represents our best fit and the colored lines show the individual contributions of the  $\pi_1$  and  $a_2$  waves.

tems where the  $a_2$ - and  $\pi_1$ -wave are directly contributing are very well described. In analogy to [20] also here a goodness of fit test has been performed for all three  $\bar{p}p$  channels by utilizing a multivariate analysis based on the concept of statistical energy [25]. The obtained p-values of 0.287, 0.490 and 0.850 for the channels  $\pi^0\pi^0\eta$ ,  $\pi^0\eta\eta$  and  $K^+K^-\pi^0$ , respectively, demonstrate that the quality of the fit is as good as the one without considering the COMPASS data yielding strong constraints for the  $\pi_1$ - and  $a_2$ -wave. In  $\pi^0\pi^0\eta$  the contribution of the  $\pi_1$ -wave with  $(12.4 \pm 0.4 \pm 6.4)\%$ , of the  $a_2$ -wave with  $(33.6 \pm 0.5 \pm 3.2)\%$  and also of all other waves are in agreement with the fractions obtained by the fit without the COMPASS data. Also the individual contributions in the channels  $\pi^0\eta\eta$  and  $K^+K^-\pi^0$  exhibit no significant differences compared to the old results.

The results for the 11 different  $\pi\pi$ -scattering data are not shown here. However, there are no major differences visible in comparison to [20].

Fig. 2 summarizes the comparison between the fit and the COMPASS data. All data can be described remarkably well. It is worth mentioning that the K-matrix of the  $\pi_1$ -wave consisting of only one pole can fairly reproduce the shapes of the intensities in  $\pi\eta$  and  $\pi\eta'$  even though there is a shift of roughly 200 MeV of the peak position between both channels (Fig. 2 (upper left) and (lower left)). A significantly worse fit result was achieved for the scenario in which the  $\pi_1$ -wave in the channel  $\bar{p}p \rightarrow \pi^0\pi^0\eta$  has been removed. The negative log-likelihood increases by more than 150 with only 20 free parameters less. Similar to the results obtained in [20] also here the  $\pi_1$ -wave is definitely needed for this  $\bar{p}p$ -annihilation channel. Contrary to the outcome without the  $\pi_1$ -wave the fit by taking into account two individual  $\pi_1$  poles does not yield significantly worse results. Based on the chosen Bayesian and Akaike information criteria [20] the two pole scenario cannot be completely excluded. A summary of all tested hypotheses with the obtained fit quality can be found in the supplemental material.

The pole positions for the individual resonances described by the K-matrix are extracted in the complex energy plane of the T-matrix on the Riemann sheet located next to the physical sheet. To some extent also partial widths have been derived from the residue calculated from the integral along a closed contour around the pole. The procedure for the extraction of these properties and also for the determination of the corresponding statistical errors based on a numerical procedure are explained in detail in [20]. The resonance parameters so obtained are summarized in Tab. I for the  $\pi_1$  pole and for the  $a_2(1320)$  and  $a_2(1700)$ . Apart from a larger width of more than 400 MeV/ $c^2$  achieved for the  $a_2(1700)$  resonance all other masses and widths are in good agreement with [20] and [21]. The absolute coupling strengths have not been determined because the non-negligible decay channel  $\rho\pi$  is not covered by the fitted data samples. Instead, the ratios  $\Gamma_{\pi\eta'}/\Gamma_{\pi\eta}$  for all three poles and  $\Gamma_{KK}/\Gamma_{\pi\eta}$  for the  $a_2$  resonances have been determined

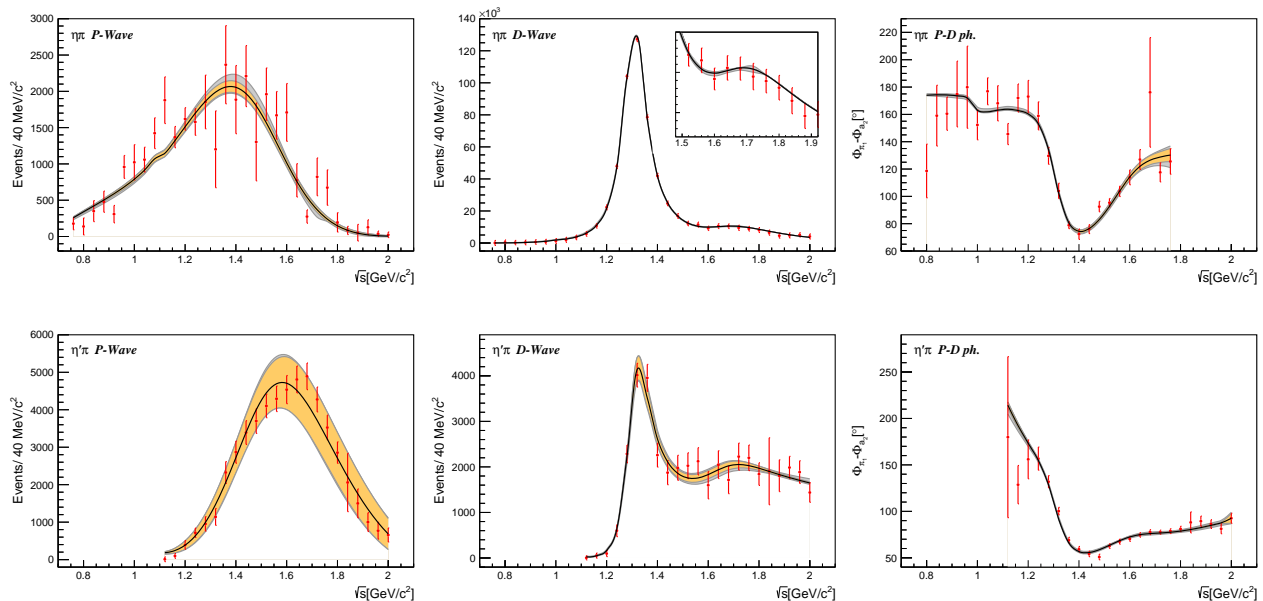


FIG. 2. Fits to the  $\eta\pi$  (upper row) and  $\eta'\pi$  (lower row) data from COMPASS. The intensities of the P (left), D wave (center), and their relative phase (right) are shown. The data are represented by the red error bars. The black line illustrates our best fit to the data, while the yellow and gray bands represent the statistical and systematic uncertainty, respectively.

TABLE I. Obtained masses, total widths and ratios of partial widths for the pole of the spin-exotic  $\pi_1$ -wave and for the two poles described in the  $a_2$ -wave, the  $a_2(1320)$  and the  $a_2(1700)$ . The statistical uncertainty is given by the first and the systematic uncertainty is provided by the second error.

name	pole mass [MeV/ $c^2$ ]	pole width [MeV]	$\Gamma_{\pi\eta'}/\Gamma_{\pi\eta}$ [%]	$\Gamma_{KK}/\Gamma_{\pi\eta}$ [%]
$a_2(1320)$	$1308.7 \pm 0.4^{+2.0}_{-4.2}$	$108.6 \pm 0.4^{+1.8}_{-12.9}$	$5.4 \pm 0.1^{+0.3}_{-0.1}$	$15.2 \pm 0.4^{+10.2}_{-3.9}$
$a_2(1700)$	$1669.2 \pm 1.0^{+20.2}_{-4.6}$	$429.0 \pm 1.7^{+44.4}_{-9.7}$	$9.0 \pm 0.1^{+8.2}_{-1.5}$	$11.7 \pm 0.5^{+87.8}_{-3.3}$
$\pi_1$	$1561.6 \pm 3.0^{+6.6}_{-2.6}$	$388.1 \pm 5.4^{+0.2}_{-14.1}$	$646.3 \pm 96.7^{+8.3}_{-50.5}$	—

which should deliver more reasonable results. The quantities for all remaining resonances, the  $K^*(892)$ ,  $\phi(1020)$ , 5  $f_0$ -, 4  $f_2$ -, 2  $a_0$ - and 2  $\rho$ -mesons, are consistent with the results obtained in [20] and are within the ballpark of other individual measurements. They are listed in the supplemental material.

#### IV. SYSTEMATIC UNCERTAINTIES

The systematic uncertainties are derived from the outcome of alternative fits which deliver reasonably good results compared to the one with the best hypothesis by applying the same criteria as in [20]. Also the impact of varying the start parameters was investigated and is included in the systematic uncertainties. In addition the effective transferred momentum squared of  $t_{eff} = -0.1 \text{ GeV}^2$  for the description of the COMPASS data has been varied in the range between  $-0.1 \text{ GeV}^2$  and  $-0.5 \text{ GeV}^2$ . Only slight differences are obtained which are also considered as systematic errors.

#### V. CONCLUSION

A coupled-channel analysis of the  $\bar{p}p$  annihilation channels  $\pi^0\pi^0\eta$ ,  $\pi^0\eta\eta$  and  $K^+K^-\pi^0$  measured at Crystal Barrel, of 11 different  $\pi\pi$ -scattering data sets and of the P- and D-waves in the  $\pi\eta$  and  $\pi\eta'$  system measured at COMPASS has been performed. The analysis was mainly focused on the investigation of the spin-exotic  $I^G(J^{PC}) = 1^-(1^+)$  wave recently observed in the  $\pi\eta$  system of the  $\bar{p}p$  channel  $\pi^0\pi^0\eta$  and in the  $\pi\eta$  and  $\pi\eta'$  system of the high energy  $\pi p$ -scattering data. For a sophisticated description of the dynamics the K-matrix approach with Chew-Mandelstam functions has been used which ensures an appropriate consideration of analyticity and unitarity conditions. The fit can reproduce all 20 different data samples reasonably well. Only one pole is needed for an appropriate description of the  $\pi_1$ -wave in the two subsystems  $\pi\eta$  and  $\pi\eta'$ , but a 2-pole scenario cannot be completely excluded. The mass and width of this single  $\pi_1$ -pole are measured to be  $(1561.6 \pm 3.0^{+6.6}_{-2.6}) \text{ MeV}/c^2$  and  $(388.1 \pm 5.4^{+0.2}_{-14.1}) \text{ MeV}$ , respectively. This result is in good agreement with [21] even though a slightly different

description for the dynamics have been chosen. The outcome of the study here confirms the statement that the two  $\pi_1$  resonances listed in the PDG, the  $\pi_1(1400)$  and  $\pi_1(1600)$ , might originate from the same pole.

## ACKNOWLEDGMENTS

The study was funded by the Collaborative Research Center under the project CRC 110: *Symmetries and the Emergence of Structure in QCD*. The authors wish to thank A. Pilloni and A. Rodas for the helpful discussions related to this work. We also gratefully acknowledge W. Dünnweber for providing important insights to the COMPASS measurement. Most of the time-consuming fits have been performed on the Green Cube at GSI in Darmstadt.

- 
- [1] P. Lacock, C. Michael, P. Boyle, and P. Rowland (UKQCD), Hybrid mesons from quenched QCD, *Phys. Lett.* **B401**, 308 (1997), arXiv:hep-lat/9611011 [hep-lat].
- [2] C. W. Bernard *et al.* (MILC), Exotic mesons in quenched lattice QCD, *Phys. Rev.* **D56**, 7039 (1997), arXiv:hep-lat/9707008 [hep-lat].
- [3] J. J. Dudek, R. G. Edwards, P. Guo, and C. E. Thomas (Hadron Spectrum), Toward the excited isoscalar meson spectrum from lattice QCD, *Phys. Rev.* **D88**, 094505 (2013), arXiv:1309.2608 [hep-lat].
- [4] A. P. Szczepaniak and E. S. Swanson, Coulomb gauge QCD, confinement, and the constituent representation, *Phys. Rev.* **D65**, 025012 (2002), arXiv:hep-ph/0107078 [hep-ph].
- [5] A. P. Szczepaniak and P. Krupinski, Energy spectrum of the low-lying gluon excitations in the Coulomb gauge, *Phys. Rev.* **D73**, 116002 (2006), arXiv:hep-ph/0604098 [hep-ph].
- [6] D. Alde *et al.* (IHEP-Brussels-Los Alamos-AnneCy(LAPP)), Evidence for a  $1^-+$  Exotic Meson, *High-energy physics. Proceedings, 24th International Conference, Munich, Germany, August 4-10, 1988*, *Phys. Lett.* **B205**, 397 (1988).
- [7] H. Aoyagi *et al.*, Study of the  $\eta\pi^-$  system in the  $\pi^-p$  reaction at 6.3-GeV/c, *Phys. Lett.* **B314**, 246 (1993), [246(1993)].
- [8] D. R. Thompson *et al.* (E852), Evidence for exotic meson production in the reaction  $\pi^-p \rightarrow \eta\pi^-p$  at 18-GeV/c, *Phys. Rev. Lett.* **79**, 1630 (1997), arXiv:hep-ex/9705011 [hep-ex].
- [9] A. Abele *et al.* (Crystal Barrel), Exotic  $\eta\pi$  state in anti-p d annihilation at rest into  $\pi^-\pi^0\eta p(\text{spectator})$ , *Phys. Lett.* **B423**, 175 (1998).
- [10] A. Abele *et al.* (Crystal Barrel), Evidence for a  $\pi\eta P$  wave in anti-p p annihilations at rest into  $\pi^0\pi^0\eta$ , *Phys. Lett.* **B446**, 349 (1999).
- [11] P. Salvini *et al.* (OBELIX), anti-p p annihilation into four charged pions at rest and in flight, *Eur. Phys. J.* **C35**, 21 (2004).
- [12] G. S. Adams *et al.* (E862), Confirmation of the  $1^-+$  meson exotics in the  $\eta\pi^0$  system, *Phys. Lett.* **B657**, 27 (2007), arXiv:hep-ex/0612062 [hep-ex].
- [13] G. S. Adams *et al.* (E852), Observation of a new  $J(PC) = 1^-+$  exotic state in the reaction  $\pi^-p \rightarrow \pi^+\pi^-\pi^-p$  at 18-GeV/c, *Phys. Rev. Lett.* **81**, 5760 (1998).
- [14] M. Alekseev *et al.* (COMPASS), Observation of a  $J^{PC} = 1^-+$  exotic resonance in diffractive dissociation of 190-GeV/c  $\pi^-$  into  $\pi^-\pi^-\pi^+$ , *Phys. Rev. Lett.* **104**, 241803 (2010), arXiv:0910.5842 [hep-ex].
- [15] E. I. Ivanov *et al.* (E852), Observation of exotic meson production in the reaction  $\pi^-p \rightarrow \eta'\pi^-p$  at 18-GeV/c, *Phys. Rev. Lett.* **86**, 3977 (2001), arXiv:hep-ex/0101058 [hep-ex].
- [16] J. Kuhn *et al.* (E852), Exotic meson production in the  $f(1)(1285)$   $\pi^-$  system observed in the reaction  $\pi^-p \rightarrow \eta\pi^+\pi^-\pi^-p$  at 18-GeV/c, *Phys. Lett.* **B595**, 109 (2004), arXiv:hep-ex/0401004 [hep-ex].
- [17] M. Lu *et al.* (E852), Exotic meson decay to  $\omega\pi^0\pi^-$ , *Phys. Rev. Lett.* **94**, 032002 (2005), arXiv:hep-ex/0405044 [hep-ex].
- [18] M. Aghasyan *et al.* (COMPASS), Light isovector resonances in  $\pi^-p \rightarrow \pi^-\pi^-\pi^+p$  at 190 GeV/c, *Phys. Rev.* **D98**, 092003 (2018), arXiv:1802.05913 [hep-ex].
- [19] C. Adolph *et al.* (COMPASS), Odd and even partial waves of  $\eta'\pi^-$  and  $\eta'\pi^-$  in  $\pi^-p \rightarrow \eta(\prime)\pi^-p$  at 191 GeV/c, *Phys. Lett.* **B740**, 303 (2015), arXiv:1408.4286 [hep-ex].
- [20] M. Albrecht *et al.* (Crystal Barrel), Coupled Channel Analysis of  $\bar{p}p \rightarrow \pi^0\pi^0\eta$ ,  $\pi^0\eta\eta$  and  $K^+K^-\pi^0$  at 900 MeV/c and of  $\pi\pi$ -Scattering Data, *Eur. Phys. J.* **C 80**, 453 (2020), arXiv:1909.07091 [hep-ex].
- [21] A. Rodas *et al.* (JPAC), Determination of the pole position of the lightest hybrid meson candidate, *Phys. Rev. Lett.* **122**, 042002 (2019), arXiv:1810.04171 [hep-ph].
- [22] D. J. Wilson, J. J. Dudek, R. G. Edwards, and C. E. Thomas (for the Hadron Spectrum Collaboration), Resonances in coupled  $\pi k, \eta k$  scattering from lattice qcd, *Phys. Rev. D* **91**, 054008 (2015).
- [23] B. Kopf, H. Koch, J. Pychy, and U. Wiedner, Partial wave analysis for  $\bar{p}p$  and  $e^+e^-$  annihilation processes, *Proceedings, 11th International Conference on Low Energy Antiproton Physics (LEAP2013): Uppsala, Sweden, June 10-15, 2013*, *Hyperfine Interact.* **229**, 69 (2014).
- [24] A. W. Jackura, *Studies in Multiparticle Scattering Theory*, Ph.D. thesis, Indiana U., Bloomington (main) (2019).
- [25] B. Aslan and G. Zech, Statistical energy as a tool for binning-free, multivariate goodness-of-fit tests, two-sample comparison and unfolding, *Nuclear Instruments and Methods in Physics Research A* **537**, 626 (2005).